An Ultrasonography Assisted Robotic HIFU Ablation Experimental System

Ching Shiow Tseng[1], Ja How Syu[1], Chi Yu An[1] and Chih-Ju Chang[1,2]
[1]*Department of Mechanical Engineering, National Central University, Jhongli, Taiwan*
[2]*Department of Neurosurgery, Cathay General Hospital, Taipei, Taiwan*

Keywords: High Intensity Focused Ultrasound, Ultrasound, Robotic, Image-guided.

Abstract: In recent years, noninvasive thermal treatment by using High Intensity Focused Ultrasound (HIFU) has high potential in tumor treatment. The goal of this research is to develop an ultrasonography assisted robotic HIFU ablation system for tumor treatment. The system integrates the technologies of ultrasound image assisted guidance, robotic positioning control, and HIFU treatment planning. With the assistance of ultrasound image guidance technology, the tumor size and location can be determined from ultrasound images and the robot can be controlled to position the HIFU probe to focus on the target tumor. An experiment of using mountain-typed template to verify the positioning accuracy of the ultrasonography assisted robotic HIFU ablation system has been done. The results show that the average positioning error is 1.06mm with a standard deviation 0.25, which is feasible for tumor therapy.

1 INTRODUCTION

Liver tumor (cancer) is a common disease. Early diagnosis and treatment of liver disease is very important measures to avoid worsening. Except biochemical tests such as GOT/GOP or α-globulin, ultrasound scanning is usually adopted for first-line screening and diagnosis. If the disease needs further treatment, tissue biopsy, percutaneous ethanol injection, or RF burning will be usually done under ultrasound guidance. For serious cases, open or minimally invasive liver dissection treatment will be necessary. However, all of them are invasive treatments. In recent years, noninvasive High Intensity Focused Ultrasound (HIFU) thermal treatment has demonstrated high potential in tumor treatment (Martinez, et al., 2012). The physical principle of this interventional approach is to apply focused ultrasound waves to the tumor tissue such that the heating of the tissue causes its necrosis (Seo, et al., 2010). Since tumors are typically much larger than the size of HIFU focal point, treatment of the entire volume of tumor is not suitable for hand-held HIFU transducer. Most of the research is conducted with the assistance of robot arm (Masamune, et al., 2013, Chauhan, 2008, Qiu, et al. 2009). Eventually, it is quite difficult to assess the quality of this non-invasive therapy, there is a dire need for a high accuracy system supporting in planning, conduction, and monitoring of such treatments. This research is aimed to study and develop an ultrasound image assisted robotic HIFU ablation system for tumor treatment (Qiu, et al., 2009]. With the assistance of ultrasound image guidance technology, ultrasound images are used to determine tumor size and location and the robot is controlled accordingly to position the focus point of a HIFU probe to the target position for thermal ablation of the tumor.

2 THE ULTRASONOGRAPHY ASSISTED ROBOTIC HIFU SYSTEM

As shown in Figure 1, the ultrasonography assisted robotic HIFU system integrates the ultrasound imaging system (ALOKA, Prosound Alpha 6), the HIFU ablation system (Sonic H-106 probe with Instek, GFG-8255 signal generator and AR, 150A100B power amplifier), the robotic arm (YAMAHA, YK400XG), the optic tracker (Northern Digital, Polaris Spectra), and a notebook (Dell, M4500) into a system.

Tseng C., Syu J., An C. and Chang C..
An Ultrasonography Assisted Robotic HIFU Ablation Experimental System.
DOI: 10.5220/0005207601090114
In *Proceedings of the International Conference on Biomedical Electronics and Devices* (BIODEVICES-2015), pages 109-114
ISBN: 978-989-758-071-0

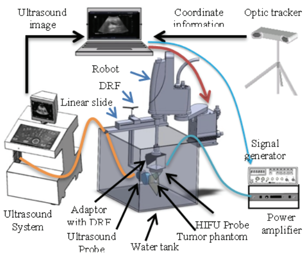

Figure 1: The ultrasonography assisted robotic HIFU system.

The ultrasound probe scans the tumor phantom to obtain the location of the tumor. The movement of the ultrasound probe is controlled by the motor-driven linear slide and detected by the optic tracker through the DRF (Dynamic Reference Frame, a tool with three IR reflective marker spheres), which is a reference coordinate frame tracked by the optic tracker. Through coordination transformation described below, the position of the tumor phantom relative to the ultrasound image frame can be transferred and represented by the robot frame. The robot is thus able to bring the focus point of the HIFU probe to aim at the tumor phantom. The signal generator and power amplifier are used to enable the HIFU probe to generate high-intensity sound power for thermal therapy.

3 COORDINATE TRANSFORMTION BETWEEN THE OPTIC TRACKER AND THE ULTRASOUND IMAGE FRAMES

Figure 2 illustrates an experimental system for determining the coordinate transformation matrix T_I^Ubetween the ultrasound probe frame (O_U) and the ultrasound image frame (O_I). A mountain-typed calibration template with three plates is fixed on the bottom of the water tank while a DRF (O_D) is also mounted on the upper corner of the water tank. The position (P_D) of the target point P (Figure 3) relative to the tank DRF frame (D) is calibrated prior to the experiment. A DRF (O_U) is also attached on the ultrasound probe for position tracking of the probe. As shown in Figure 3, the middle plate of the calibration template is scanned by the ultrasound probe and the image coordinate (P_I) of the target point P is determined from the ultrasound image. The position of the target point P relative to the optic tracker frame can be expressed through either the tank DRF frame or the ultrasound probe frame as shown in equation (1).

$$T_D^T P_D = T_U^T T_I^U P_I \tag{1}$$

where I represents ultrasound image frame
U represents ultrasound probe frame
T represents optic tracker frame
D represents the tank DRF frame
T_D^T, T_U^T, P_D and P_I are known.

The transformation matrix T_I^U can be determined by bringing the tracker and image coordinates of the target point P at three or more positions, P_i (P_{Di} 、P_{Ii}), i=1, 2,…N, N≥3 into equation (1) and solved by optimization method such as the least square algorithm. After the transformation matrix T_I^U has been determined, the coordinates of any target tumor detected by ultrasound scan (Figure 5) can be transferred and expressed relative to the optic tracker frame as described by equation (2).

$$P_T = T_U^T\, T_I^U\, P_I \tag{2}$$

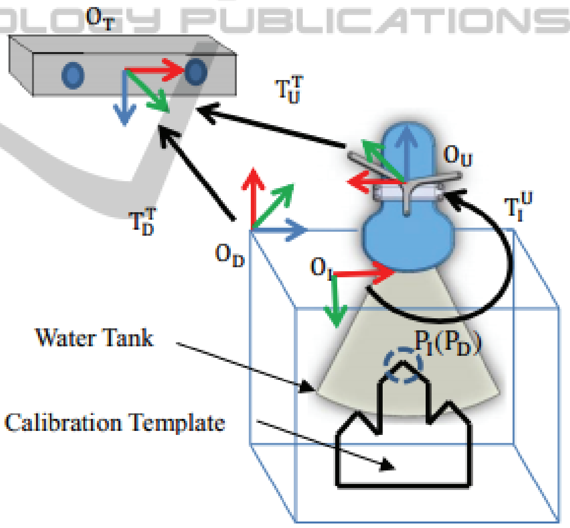

Figure 2: The coordinate transformation among all frames for the registration of the optic tracker and the ultrasound image.

The calibration template used for the registration of the optic tracker frame and the ultrasound image frame is shown in Figure 3. Since ultrasound scan beam has a slice thickness (elevational direction), it is necessary to determine the middle plane of the slice so that the following positioning calibration will be more precise. Therefore, a three-layer template is designed to make sure that the ultrasound scan is correctly located on the middle plate which will have brighter or clear boundary images than the other two plates.

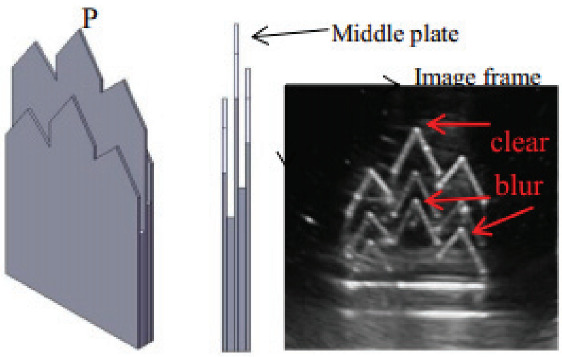

Figure 3: The calibration template and the boundary image of the middle plate, which is clearer than those of the other two plates.

4 COORDINATE TRANSFORMATION BETWEEN THE ROBOT AND THE ULTRASOUND SYSTEM

Figure 4 shows the coordinate transformation relationship between the optic tracker and the robot. A tracking device mounted with a DRF (coordinate frame E) and a pin of 10cm in length (tip point P represents the focus point of the HIFU transducer) is designed and mounted at the end effector of the robot. A DRF is fixed on the robot base and used to define the world coordinate frame W in case the optic tracker is moved during the experiment. The robot coordinate frame is defined as frame R. The transformation matrix T_W^T and T_E^T can be determined directly by the optic tracker. The transformation matrix T_W^R is to be solved so that the coordinates relative to the optic tracker frame can be transformed relative to the robot frame. In other words, the coordinates of any target point determined by the ultrasound scan can be transformed to those relative to the robot frame through the optic tracker.

The position of the origin of the coordinate frame E, O_E , can be described relative to the coordinate frame W as below.

$$O_W = \left(T_W^T\right)^{-1} T_E^T O_E \tag{3}$$

If the robot is manipulated to move around, the coordinates of point O_E relative to the coordinate frames R and W are calculated by the robot controller and equation (3) respectively. Therefore, the transformation matrix T_W^R between the robot and optic tracker can be determined by equation (4).

$$O_R = T_W^R O_W \tag{4}$$

Because both O_W and O_R are not square matrices (4x1), we use least mean square algorithm to solve T_W^R.

$$T_W^R = O_R {O_W}^T \left(O_W {O_W}^T\right)^{-1} \tag{5}$$

After completion of the registrations between the ultrasound image and the optic tracker and between the optic tracker and the robot, the coordinates of the target tumor scanned and detected by the ultrasound system can be transformed and represented by the robot frame. The transformation is defined by Eq. (6) and illustrated by Figure 5.

$$P_R = T_W^R T_T^W T_U^T T_I^U P_I \tag{6}$$

where P_I: Image coordinate of the target tumor

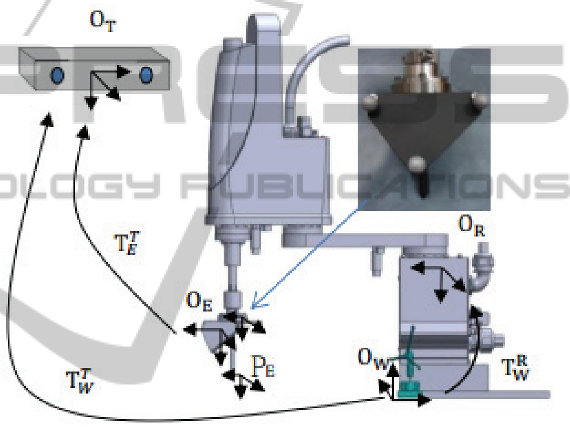

Figure 4: The coordinate transformation between the optic tracker and the robot.

Figure 5 also shows that the HIFU transducer has been mounted to the end effector of the robot for HIFU thermal treatment.

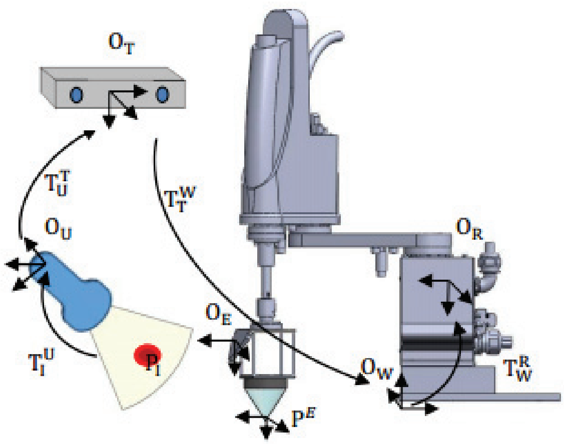

Figure 5: The coordinate transformation between the tumor P_I and the robot.

The procedures of the HIFU thermal ablation of the ultrasonography assisted robotic HIFU system is described in the flow chart of Figure 6.

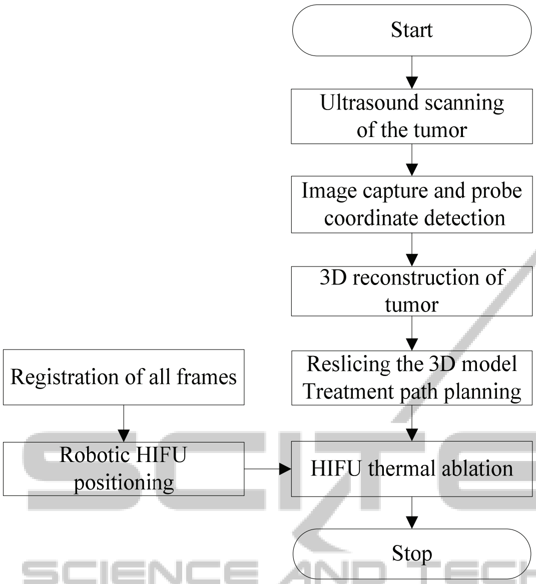

Figure 6: The procedure of thermal ablation of the robotic HIFU system.

5 EXPERIMENT AND DISCUSSION

5.1 Position Measure of the Target

An experiment has been conducted to verify the position measure error through the coordinate transformation between the ultrasound image and the optic tracker frames. The mountain-type template was seated in depth of 3cm, 7cm and 12cm. The template in each depth was scanned three times by the ultrasound probe. The positioning error is defined as the difference between the image coordinate of the target point after coordinate transformation and the coordinate measured directly by the optic tracker. The average positioning error of the three peak points of the template in depth of 3cm, 7cm and 12cm are 1.49mm, 1.46mm and 2.15mm respectively. Table 1 listed the experiment data of the case in 7cm depth.

5.2 Positioning of the Robot Arm

The robot was commanded to move around to ten positions to calculate the transformation matrix T_W^R by Eq. (5). After that, the calibration template of Figure 3 seated in depth 7cm was scanned by the ultrasound. Then the robot was command to move the pinpoint P (Figure 4) of the rod to the three peak points of the template as shown in Figure 7. The distance errors between the peak points and the pinpoint P are listed in Table 2. The positioning error is 1.06±0.25mm.

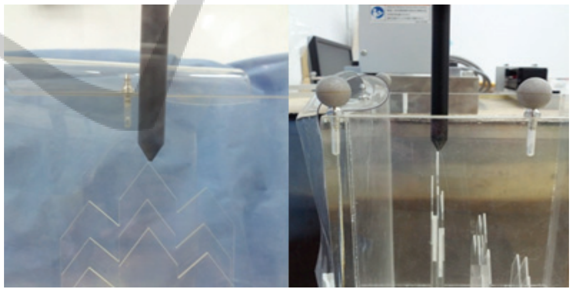

Figure 7: The pinpoint of the rod positions to the peak point of the calibration template.

Table 1: Distance error of the phantom in 7cm depth.

No. of point	Coordinate of the target point			No. of Image	Coordinates of the guided pinpoint			Distance error
	x	y	z		x	y	z	
1	38.9	27.9	-89.5	I	39.1	28.0	-90.5	-0.24
				II	39.1	28.0	-90.7	-0.17
				III	39.5	27.8	-90.5	-0.62
2	18.3	14.0	-87.7	I	18.0	13.6	-88.1	0.27
				II	17.4	13.8	-88.5	0.83
				III	18.1	13.9	-88.1	0.18
3	13.7	-0.1	-104.5	I	14.0	-0.5	-105.4	-0.28
				II	14.2	-0.2	-105.5	-0.46
				III	14.0	-0.0	-105.8	-0.29
Max error		1.38	Average error		1.01	Standard deviation		0.26

Table 2: Positioning error of the robot arm.

No. of point	Coordinate of the target point			No. of Image	Coordinate of the guided pinpoint			Distance error
	x	y	z		x	y	z	
1	38.9	27.9	-89.8	I	39.2	27.8	-90.6	1.04
				II	39.2	27.9	-90.6	1.10
				III	39.6	27.7	-90.5	1.16
2	18.3	14.0	-87.7	I	18.1	13.5	-88.2	0.79
				II	17.5	13.7	-88.5	1.19
				III	18.2	13.8	-88.1	0.50
3	13.7	-0.1	-104.5	I	14.0	-0.6	-105.5	1.16
				II	14.2	-0.4	-105.6	1.23
				III	14.0	-0.1	-105.9	1.40
Max error		1.4	Average error		1.06	Standard deviation		0.25

Table 3: Positioning error of HIFU thermal ablation.

No. of points	Position of the target (mm)			Position of the ablation (mm)			Distance error
	X	Y	Z	X	Y	Z	
1	-71.6	248.6	79.7	-71.4	248.2	80.0	0.5
2	-70.6	289.2	81.2	-72.6	288.6	81.1	2.1
3	-112.0	248.4	79.63	-111.0	248.1	79.7	1.0
4	-109.0	289.5	81.24	-108.0	288.7	80.3	1.6

5.3 Positioning of HIFU Ablation

The ultrasonography assisted robotic HIFU treatment experiment was conducted by commanding the robot to move HIFU focus point to ablate the four corner points of a phantom, which was detected by ultrasound images. Figure 8 shows the HIFU focus point can be positioned to the target (corner) points for thermal ablation. The average positioning error is 1.3±0.8mm and the distance error of each corner point is listed in Table 3.

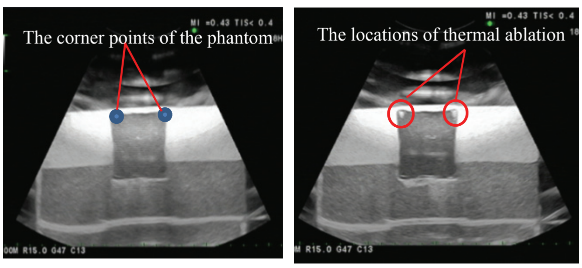

Figure: 8: Positioning experiment of the HIFU thermal ablation.

6 CONCLUSIONS

This study proposes an ultrasonography assisted robotic HIFU system for thermal ablation of tumor. The position coordinates of targets determined by the ultrasound image are transformed to the robot coordinate frames so that the robot can move the HIFU probe to focus on the targets. The experiment results show that positioning errors of the robotic HIFU system is accurate enough for thermal ablation treatment of tumor tissue. Since robots have great dynamic response in motion, it is highly possible to apply the robotic HIFU system to treat live tumors in the future, which requires the compensation of movement due to respiration.

ACKNOWLEDGEMENTS

The authors would like to thank for the financial support from Ministry of Science and Technology, Taiwan, under the contract of NSC 101-2221-E-008-020-MY3.

REFERENCES

Masamune, K., Kurima, I., Kuwana, K., et al., 2013, HIFU Positioning Robot for Less-Invasive Fetal Treatment, Procedia CIRP, vol. 5, , pp. 286-289.

Chauhan, S., 2008, FUSBOTs: Image-guided Robotic Systems for Focused Ultrasound Surgery, Medical Robotics, Vanja Bozovic, ISBN 978-3-902613-18-9, *I-Tech Education and Publishing*, Vienna, Austriap, pp.526.

Chauhan, S. Tan, M.T., Seet, G., et al., 2009, Minimally invasive robotic HIFU neurosurgical applications, in *38th Annual Symposium of the Ultrasonic Industry Association (UIA), , Vancouver, BC*, pp. 1-5.

Qiu, Z. Gao, J., Cochran, S., et al., 2009, The development of therapeutic ultrasound with assistance of robotic manipulator," *Proc IEEE Eng Med Biol Soc*, pp. 733-736.

Seo, J., Koizumi, N., Yoshinaka, N., et al., 2010, Three-dimensional computer-controlled acoustic pressure scanning and quantification of focused ultrasound, *IEEE Trans Ultrason Ferroelectr Freq Control*, vol. 57, pp. 883-891.

Martinez, R., Vera, A. and Leija, L., 2012, High-intensity focused ultrasound thermal mapping by using a thermocouple embedded in a tissue-mimicking material, Electrical Engineering, Computing Science and Automatic Control (CCE), *9th International Conference*, pp. 1-4.

Soneson, J.E., 2009, A User-Friendly Software Package for HIFU Simulation, *AIP Conference Proceedings*, Vol. 1113 Issue 1, p165.

Chauhan, S., 2008, Image-guided Robotic Systems for FUS (Focused Ultrasound Surgery), Vanja Bozovic, ISBN 978-3-902613-18-9, *I-Tech Education and Publishing, Vienna, Austriap*, pp.526.

Qiu, Z., Gao, J., Cochran, S., et al. 2009, The development of therapeutic ultrasound with assistance of robotic manipulator, *Proc IEEE Eng Med Biol Soc*, pp. 733-736.

Hill, C.R., Rivens, L., Vaughan, M.G., et al., 1994, Lesion development in focused ultrasound surgery: A general model, *Ultrasound in Medicine & Biology*, vol. 20, pp. 259-269.

Takegami, K., Kaneko, Y., Watanabe, T., et al., 2004, Polyacrylamide gel containing egg white as new model for irradiation experiments using focused ultrasound," *Ultrasound Med Biol*, vol. 30, pp. 1419-1422.

Tung, Y.S., Liu, H.L., Wu, C.C., et al., 2006, Contrast-agent enhanced ultrasound thermal ablation," *Ultrasound Med Biol*, vol. 32, pp. 1103-1110.

Luo, H., Shen, G., and Chen, Y., 2009, Treatment Planning of Scanning Time and Path for Phased High-Intensity Focused Ultrasound Surgery, in *Biomedical Engineering and Informatics*, BMEI '09. , pp. 1-4.

Vaezy, S., Shi, X., Martin, R.W., et al., 2001, Real-time visualization of high-intensity focused ultrasound treatment using ultrasound imaging, *Ultrasound in Medicine & Biology*, vol. 27, pp. 33-42.

Sakuma, I., Takai, Y., Kobayashi, E., et al., 2002, Navigation of High Intensity Focused Ultrasound Applicator with an Integrated Three-Dimensional Ultrasound Imaging System, *MICCAI, 5th International Conference*, vol. 2489, pp. 133-139.